Hindawi
Advances in High Energy Physics
Volume 2019, Article ID 6034981, 14 pages
https://doi.org/10.1155/2019/6034981

Research Article

Contributions of Jets in Net Charge Fluctuations from the Beam Energy Scan at RHIC and LHC

Bushra Ali, Shaista Khan, and Shakeel Ahmad

Department of Physics, Aligarh Muslim University, Aligarh 202 002, India

Correspondence should be addressed to Shakeel Ahmad; shakeel.ahmad@cern.ch

Received 18 March 2019; Accepted 13 June 2019; Published 14 July 2019

Academic Editor: Fu-Hu Liu

Dynamical net charge fluctuations have been studied in ultrarelativistic heavy-ion collisions from the beam energy scan at RHIC and LHC energies by carrying out the hadronic model simulation. Monte Carlo model, HIJING, is used to generate events in two different modes, HIJING-default with jet quenching switched off and jet/minijet production switched off. A popular variable, $\nu_{[+-,dyn]}$, is used to study the net charge fluctuations in different centrality bins and the findings are compared with the available experimental values reported earlier. Although the broad features of net charge fluctuations are reproduced by the HIJING, the model predicts the larger magnitude of fluctuations as compared to the one observed in experiments. The role of jets/minijets production in reducing the net charge fluctuations is, however, distinctly visible from the analysis of the two types of HIJING events. Furthermore, $dN_{ch}/d\eta$ and $1/N$ scaling is partially exhibited, which is due to the fact that, in HIJING, nucleus-nucleus collisions are treated as multiple independent nucleon-nucleon collisions.

1. Introduction

The interest in the studies involving event-by-event fluctuations in hadronic (hh) and heavy-ion (AA) collisions is primarily connected to the idea that the correlations and fluctuations of dynamical origin are associated with the critical phenomena of phase transitions and leads to the local and global differences between the events produced under similar initial conditions [1, 2]. Several different approaches have been made to investigate the event-by-event fluctuations in hh and AA collisions at widely different energies, for example, multifractals [3–5], normalized factorial moments [6], erraticity [4, 7], k-order pseudorapidity spacing [8, 9], and transverse momentum(p_T) spectra. Furthermore, event-by-event fluctuations in the conserved quantities, like strangeness, baryon number, and electric charge, have emerged as new tools to estimate the degree of equilibration and criticality of the measured system [10]. Experiments such as RHIC and LHC are well suited for the study of these observables [10, 11].

Event-by-event fluctuations of net charge of the produced relativistic charged particles serve as an important tool to investigate the composition of hot and dense matter prevailing in the "fireball", created during the intermediate stage of AA collisions, which, in principle, can be characterized in the framework of QCD [11]. It has been argued that a phase transition from QGP to normal hadronic state is an entropy conserving process [12] and, therefore, the fluctuations in net electric charge will be significantly reduced in the final state in comparison to what is envisaged to be observed from a hadron gas system [13, 14]. This is expected because the magnitude of charge fluctuations is proportional to the square of the number of charges present in the system which depends on the state from which charges originate. In a system passing through QGP phase, quarks are the charge carriers, whereas in the case of hadron gas, the charge carriers are hadrons. This suggests that the charge fluctuations observed in the case of QGP with fractional charges would be smaller than those in hadron gas with integral charges [10, 15, 16]. A reduction in the fluctuations of net charge in Pb-Pb collision at $\sqrt{s_{NN}} = 2.76$ TeV in comparison to that observed at RHIC has been reported by ALICE collaboration [17]. A question arises here whether the fluctuations arising from QGP or from hadron gas would survive during the evaluation of the system [10, 18–21]. The fluctuations observed at the freeze-out depend crucially on the equation of state of the system and final effects. It has been shown [22] that large charge fluctuations survive, if they are accompanied by large temperature fluctuations at freeze-out in context to the experiments. Measurement of charge fluctuations depends on the observation window, which is so selected that the majority of the fluctuations are captured without being affected by the conservation limits [19–21].

An attempt is, therefore, made to carry out a systematic study of dynamical net charge fluctuations from beam energy scan at RHIC and LHC energies using the Monte Carlo model, HIJING, and the findings are compared with those obtained with the real data and other MC models. The reason for using the code HIJING is that it gives an opportunity to study the effect of jets and jet-quenching. HIJING events are generated at various beam energies corresponding to RHIC and LHC which cover an energy range from $\sqrt{s_{NN}}$ = 62.4 GeV to 5.02 TeV. Two sets of events, (i) HIJING-default with jets and minijets and (ii) HIJING with no jet/minijet production, are generated for each of the incident energies considered.

2. Formalism

The charge fluctuations are usually studied in terms of two types of measures [23]. The first one is D, which is the direct measure of the variance of event-by-event net charge $\langle \delta Q^2 \rangle = \langle Q^2 \rangle - \langle Q \rangle^2$, where $Q = N_+ - N_-$; N_+ and N_-, respectively, denote the multiplicities of positively and negatively charged particles produced in an event in the considered phase space. Since the net charge fluctuations may get affected by the uncertainties arising out of volume fluctuations, the fluctuations in the ratio $R = N_+/N_-$ are taken as the other suitable parameter. R is related to the net charge fluctuations via the parameter D as [13, 15–17]

$$D = \langle N_{ch} \rangle \delta R^2 \simeq 4 \frac{\langle \delta Q^2 \rangle}{\langle N_{ch} \rangle} \tag{1}$$

which gives a measure of charge fluctuations per unit entropy. It has been shown that D acquires a value ~4 for an uncorrelated pion gas which decreases to ~3 after taking into account the resonance yields [15]. For QGP, the value of D has been reduced to ~ 1 − 1.5, where the uncertainty arises due to the uncertainties involved in relating the entropy to the multiplicity of the charged hadrons in the final state [24]. The parameter D, thus, may be taken as an efficient probe for distinguishing between the hadron gas and QGP phases. These fluctuations are, however, envisaged to be diluted in the rapidly expanding medium due to the diffusion of particles in rapidity space [19, 20]. Resonance decays, collision dynamics, radial flow, and final state interactions may also affect the amount of fluctuations measured [15, 25–27]. The first results on net charge fluctuations at RHIC were presented by PHENIX [28] in terms of reduced variance $\omega_d = \langle \delta Q^2 \rangle / N_{ch}$, while STAR [27] results were based on a dynamical net charge fluctuations measure, $\nu_{[+-,dyn]}$, and were treated as a rather reliable measure of the net charge fluctuations as $\nu_{[+-,dyn]}$ was found to be robust against detection efficiency.

Furthermore, the contributions from statistical fluctuations would also be present if net charge fluctuations are studied in terms of parameter D and it will be difficult to extract the contribution due to fluctuations of dynamical origin. The novel method of estimating the net charge fluctuations takes into account the correlation strength between + +, - -, and + - charge particle pairs [10, 29]. The difference between the relative multiplicities of positively and negatively charged particles is given as

$$\nu_{+-} = \left\langle \left(\frac{N_+}{\langle N_+ \rangle} - \frac{N_-}{\langle N_- \rangle} \right)^2 \right\rangle \tag{2}$$

where the angular brackets represent the mean value over the entire sample of events. The Poisson limit of this quantity is expressed as [27]

$$\nu_{[+-,stat]} = \frac{1}{\langle N_+ \rangle} + \frac{1}{\langle N_- \rangle} \tag{3}$$

The dynamical net charge fluctuations may, therefore, be written as the difference of these two quantities:

$$\nu_{[+-,dyn]} = \nu_{[+-]} - \nu_{[+-,stat]} \tag{4}$$

$$\begin{aligned} \nu_{[+-,dyn]} = {} & \frac{\langle N_+ (N_+ - 1) \rangle}{\langle N_+ \rangle^2} + \frac{\langle N_- (N_- - 1) \rangle}{\langle N_- \rangle^2} \\ & - 2 \frac{\langle N_+ N_- \rangle}{\langle N_+ \rangle \langle N_- \rangle} \end{aligned} \tag{5}$$

From the theoretical point of view, $\nu_{[+-,dyn]}$ can be expressed in terms of two particle integral correlation functions as

$$\nu_{[+-,dyn]} = R_{++} + R_{--} - 2R_{+-} \tag{6}$$

where the term $R_{\alpha\beta}$ gives the ratio of integrals of two- and single-particle pseudorapidity density function, defined as

$$R_{\alpha\beta} = \frac{\int dn_\alpha dn_\beta \left(dN/dn_\alpha dn_\beta \right)}{\int dn_\alpha \left(dN/dn_\alpha \right) \int dn_\beta \left(dN/dn_\beta \right)} \tag{7}$$

The variable $\nu_{[+-,dyn]}$ is, thus, basically a measure of relative correlation strength of + +, - -, and + - charged hadron pairs. For independent emission of particles, these correlations should be ideally zero. However, in practice, a partial correlation is observed due to string and jet-fragmentation, resonance decays, and so forth. The strengths of R_{++}, R_{--}, and R_{+-} are expected to vary with system size and beam energy. Moreover, as the charge conservation, + - pair are expected to be rather strongly correlated as compared to like sign charge pairs and hence $2R_{+-}$ in (6) is envisaged to be larger than the sum of the other two terms [27] giving $\nu_{[+-,dyn]}$ values less than zero, which is evident from the results based on pp and $\overline{p}p$ collisions at CERN ISR and FNAL and later on in heavy-ion collisions at RHIC [27, 29–32] and LHC energies [17, 27].

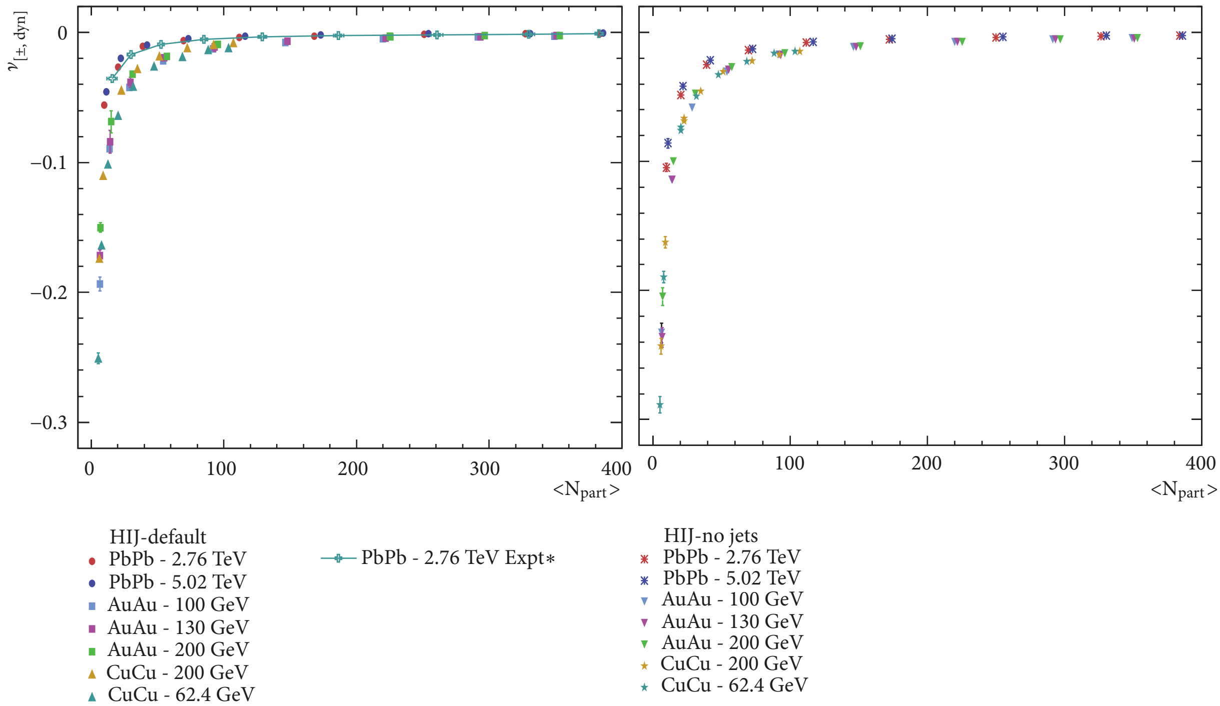

FIGURE 1: Dependence of net charge fluctuations $\nu_{[+-,dyn]}$ on the number of participating nucleons, N_{part}, for the HIJING events with jets/minijets on and off. Experimental results for Pb-Pb collisions at 2.76 TeV are also shown [data from [17]].

TABLE 1: Details of events selected for analysis.

Energy (GeV)	Type of collision	No. of events ($\times 10^6$)
5020	Pb-Pb	0.6
2760	Pb-Pb	0.6
200	Au-Au	0.6
130	Au-Au	0.6
100	Au-Au	0.6
200	Cu-Cu	1.0
62.4	Cu-Cu	1.0

3. Results and Discussion

Several sets of MC events corresponding to different collision systems in a wide range of beam energies are generated using the code HIJING- 1.37 [33] for the present analysis. The details of the events simulated are listed in Table 1. Two sets of events for each beam energy and colliding nuclei, HIJING-default with jet-quenching off and with jet/minijet production switched off, are simulated and analyzed. It has been argued [34, 35] that the minijets (semihard parton scattering with few GeV/c momentum transfer) are copiously produced in the early state of AA collisions at RHIC and higher energies. In a QGP medium, if present, the jets/minijets will lose energy through induced gluon radiation [36], a process referred to as jet-quenching in the case of higher p_T partons. The properties of the dissipative medium would determine the extent of energy loss of jets and minijets. The influence of the production of jets/minijets in AA collisions in the produced medium on the net charged fluctuations may be investigated by comparing the findings due to the two types of HIJING simulated events. The analysis has been carried out by considering the particles having their pseudorapidity values $|\eta| < 1.0$ and p_T values in the range 0.2 GeV/c $< p_T <$ 5.0 GeV/c. These η and p_T cuts have been applied to facilitate the comparison of the findings with the experimental result having similar cuts.

Values of $\nu_{[+-,dyn]}$ for different collision centralities are estimated for various data sets and are listed in Tables 2–5 along with the corresponding values of number of participating nucleons, N_{part}. Variations of $\nu_{[+-,dyn]}$ with mean number of participating nucleons, N_{part}, for various data sets are exhibited in Figure 1. Such dependencies observed in experiments STAR [27] and ALICE [17, 32] are also displayed in the same figure. A monotonic dependence of $\nu_{[+-,dyn]}$ on N_{part} is seen in the figure. It may be of interest to note that, for a given N_{part}, the magnitude of $\nu_{[+-,dyn]}$ decreases with increasing beam energy and this difference becomes more and more pronounced on moving from most central (5%) to the peripheral (70 − 80%) collisions. It is also interesting to note in the figure that the HIJING predicted values (for HIJING-default events) are quite close to the experimental values. However, the corresponding $\nu_{[+-,dyn]}$ values for the events with jets/minijets off are somewhat larger. The jets-off multiplicities reflect the soft processes, whereas the jets-on multiplicities include the contributions from the jets and minijets [32]. This may cause the reduction in the contributions coming from the third term of (5), which represents the correlations between + - pairs. This is expected to occur at these energies, as the events have high multiplicities and are dominated by multiple minijet productions, which might

TABLE 2: Values of N_{part}, $\nu_{[+-,dyn]}$, and $\nu^{corr}_{[+-,dyn]}$ for various centrality classes in $|\eta| < 1$ for events corresponding to $^{197}Au - ^{197}Au$ collisions.

	HIJING-default			HIJING-no jets		
cent.%	N_{part}	$\nu_{[+-,dyn]}$	$\nu^{corr}_{[+-,dyn]}$	N_{part}	$\nu_{[+-,dyn]}$	$\nu^{corr}_{[+-,dyn]}$
Au-Au at 100 GeV errors are in units of $\times 10^{-3}$						
5	349.19±0.10	-0.00279±0.06	-0.00134±0.67	349.36±0.10	-0.00450±0.11	-0.00247±1.23
10	291.43±0.10	-0.00339±0.07	-0.00162±0.81	291.54±0.10	-0.00523±0.14	-0.00278±1.39
20	219.88±0.10	-0.00469±0.07	-0.00228±1.14	219.95±0.10	-0.00743±0.15	-0.00418±2.09
30	146.36±0.08	-0.00742±0.12	-0.00373±1.87	146.21±0.08	-0.01137±0.21	-0.00647±3.24
40	91.66±0.07	-0.01252±0.22	-0.00643±3.22	91.79±0.07	-0.01735±0.41	-0.00955±4.78
50	54.16±0.05	-0.02176±0.35	-0.01126±5.63	54.00±0.05	-0.03048±0.56	-0.01725±8.63
60	28.81±0.04	-0.04201±0.82	-0.02183±10.9	28.72±0.04	-0.05813±1.06	-0.03342±16.72
70	13.73±0.02	-0.08949±1.37	-0.04683±23.42	13.76±0.02	-0.11431±2.79	-0.06308±31.58
80	6.51±0.02	-0.19365±5.40	-0.10322±51.69	6.48±0.02	-0.23294±7.70	-0.12489±62.58
Au-Au at 130 GeV errors are in units of $\times 10^{-3}$						
5	350.57±0.10	-0.00238±0.06	-0.00116±0.58	350.56±0.10	-0.00466±0.10	-0.00276±1.38
10	293.23±0.10	-0.00306±0.06	-0.00156±0.78	293.29±0.10	-0.00531±0.16	-0.00303±1.52
20	221.67±0.10	-0.00424±0.61	-0.00219±1.14	222.00±0.10	-0.00722±0.19	-0.00420±2.10
30	147.80±0.08	-0.00666±0.77	-0.00351±1.80	147.97±0.08	-0.01109±0.20	-0.00657±3.28
40	93.12±0.07	-0.01093±3.68	-0.00571±3.44	93.16±0.07	-0.01741±0.38	-0.01025±5.13
50	55.14±0.05	-0.01936±2.35	-0.01030±5.30	55.08±0.05	-0.02889±0.61	-0.01683±8.42
60	29.49±0.04	-0.03832±3.89	-0.02091±10.66	50.10±0.05	-0.02884±0.70	-0.01683±8.43
70	14.14±0.03	-0.08413±8.79	-0.04713±24.07	14.23±0.03	-0.11416±2.80	-0.06826±34.17
80	6.71±0.02	-0.17158±4.41	-0.09314±46.63	6.74±0.02	-0.23619±7.59	-0.13987±70.08
Au-Au at 200 GeV errors are in units of $\times 10^{-3}$						
5	353.05±0.09	-0.00216±0.05	-0.00120±0.60	353.17±0.09	-0.00452±0.11	-0.00279±1.39
10	296.71±0.10	-0.00255±0.04	-0.00138±0.69	296.84±0.10	-0.00544±0.14	-0.00337±1.69
20	225.37±0.10	-0.00317±0.31	-0.00160±0.81	225.55±0.10	-0.00723±0.12	-0.00450±2.25
30	155.03±0.10	-0.00557±0.42	-0.00100±0.52	151.28±0.08	-0.01067±0.18	-0.00662±3.31
40	95.63±0.07	-0.00917±1.00	-0.00505±2.58	96.00±0.07	-0.01630±0.28	-0.00993±4.97
50	56.92±0.05	-0.01855±2.54	-0.01129±5.85	57.39±0.05	-0.02718±0.52	-0.01657±8.29
60	31.07±0.04	-0.03223±6.21	-0.01850±9.26	31.16±0.04	-0.04752±0.99	-0.028104±14.06
70	14.93±0.03	-0.06861±8.52	-0.03957±20.38	15.12±0.03	-0.09972±2.23	-0.059954±30.00
80	7.16±0.02	-0.15018±3.64	-0.08783±43.97	7.18 ±0.02	-0.20465±6.96	-0.121323±60.80

Table 3: Values of N_{part}, $\nu_{[+-,dyn]}$, and $\nu^{corr}_{[+-,dyn]}$ for different centrality bins in $|\eta| < 1.0$ simulated for $^{64}Cu - {}^{64}Cu$ interactions at 62.4 and 200 GeV.

	HIJING-default			HIJING-no jets		
cent.%	N_{part}	$\nu_{[+-,dyn]}$	$\nu^{corr}_{[+-,dyn]}$	N_{part}	$\nu_{[+-,dyn]}$	$\nu^{corr}_{[+-,dyn]}$
Cu-Cu at 62.4 GeV errors are in units of $\times 10^{-3}$						
5	103.68±0.03	-0.011595±0.26	-0.00519±2.60	103.73±0.03	-0.01479±0.36	-0.00725±3.62
10	88.36±0.04	-0.01314±0.23	-0.00556±2.78	88.45±0.04	-0.01631±0.43	-0.00743±3.72
20	68.59±0.04	-0.01813±0.31	-0.00825±4.12	68.35±0.04	-0.02268±0.37	-0.01115±5.57
30	47.57±0.03	-0.02577±0.44	-0.01134±5.67	47.61±0.03	-0.03284±0.48	-0.01623±8.12
40	31.62±0.03	-0.04126±0.52	-0.01937±9.69	31.58±0.03	-0.04972±0.75	-0.02466±12.34
50	20.45±0.02	-0.06349±1.16	-0.02943±14.72	20.42±0.02	-0.07580±1.09	-0.03711±18.56
60	12.67±0.02	-0.10112±2.01	-0.04593±22.98	19.33±0.02	-0.07352±1.31	-0.03464±17.33
70	7.92±0.01	-0.16345±2.73	-0.07501±37.53	7.91±0.01	-0.18968±4.29	-0.09017±45.13
80	5.26±0.01	-0.25073±4.09	-0.11766±58.86	5.28±0.01	-0.28850±6.42	-0.13992±70.03
Cu-Cu at 200 GeV errors are in units of $\times 10^{-3}$						
5	107.26±0.03	-0.00756±0.16	-0.00423±2.12	107.09±0.03	-0.01468±0.45	-0.00905±4.53
10	92.39±0.04	-0.00911±0.17	-0.00517±2.58	92.31±0.04	-0.01728±0.43	-0.01073±5.37
20	72.41±0.04	-0.01174±0.18	-0.00648±3.24	72.54±0.04	-0.02189±0.46	-0.01355±6.78
30	51.26±0.03	-0.01766±0.25	-0.00997±4.98	51.31±0.03	-0.03018±0.56	-0.01839±9.20
40	34.79±0.03	-0.02786±0.39	-0.01613±8.06	34.82±0.03	-0.04548±0.96	-0.02814±14.08
50	22.92±0.03	-0.04417±0.77	-0.02579±12.90	22.88±0.03	-0.06879±1.45	-0.04248±20.12
60	20.93±0.03	-0.04410±0.64	-0.02579±12.90	20.91±0.03	-0.06650±1.33	-0.04027±21.01
70	9.11±0.02	-0.10984±2.26	-0.06197±31.01	9.13±0.02	-0.16262±4.29	-0.09710±48.62
80	5.99±0.01	-0.17367±2.84	-0.10029±50.17	5.98±0.01	-0.24322±6.05	-0.14339±71.78

Table 4: Values of N_{part}, $\nu_{[+-,dyn]}$, and $\nu^{corr}_{[+-,dyn]}$ for different centrality bins in $|\eta| < 1.0$ simulated for $^{208}Pb - ^{208}Pb$ collisions at 2.76 and 5.02 TeV.

cent.%	HIJING-default N_{part}	HIJING-default $\nu_{[+-,dyn]}$	HIJING-default $\nu^{corr}_{[+-,dyn]}$	HIJING-no jets N_{part}	HIJING-no jets $\nu_{[+-,dyn]}$	HIJING-no jets $\nu^{corr}_{[+-,dyn]}$
			Pb-Pb at 2760 GeV errors are in units of $\times 10^{-3}$			
5	383.54±0.09	-0.00077±0.01	-0.00055±0.27	383.75±0.09	-0.00227±0.06	-0.00160±0.80
10	327.34±0.11	-0.00091±0.02	-0.00062±0.31	333.39±1.77	-0.00279±0.06	-0.00200±1.00
20	250.99±0.11	-0.00124±0.01	-0.00085±0.42	249.97±0.11	-0.00385±0.05	-0.00282±1.41
30	168.17±0.09	-0.00269±0.03	-0.00196±0.98	172.23±0.09	-0.00517±0.10	-0.00367±1.83
40	115.74±0.08	-0.00354±0.04	-0.00251±1.25	111.91±0.08	-0.00803±0.15	-0.00571±2.85
50	69.43±0.09	-0.00640±0.14	-0.00461±2.30	69.52±0.06	-0.01373±0.26	-0.00997±4.99
60	31.13±0.04	-0.01060±0.62	-0.00722±3.63	39.36±0.05	-0.02487±0.38	-0.01815±9.08
70	22.33±0.04	-0.02685±0.31	-0.01943±9.71	20.33±0.03	-0.04836±0.93	-0.03506±17.54
80	11.25±0.04	-0.05571±0.87	-0.03928±19.65	9.99±0.03	-0.10468±3.34	-0.07691±38.53
			Pb-Pb at 5020 GeV errors are in units of $\times 10^{-3}$			
5	385.67±0.09	-0.00056±0.01	-0.00040±0.20	386.00±0.09	-0.00225±0.06	-0.00167±0.83
10	331.10±0.11	-0.00077±0.01	-0.00057±0.28	330.62±0.11	-0.00257±0.06	-0.00189±0.94
20	254.11±0.11	-0.00093±0.01	-0.00064±0.32	255.20±0.11	-0.00355±0.06	-0.00267±1.33
30	173.09±0.12	-0.00164±0.01	-0.00129±0.64	174.31±0.09	-0.00515±0.07	-0.00385±1.92
40	116.08±0.08	-0.00277±0.03	-0.00205±1.02	116.85±0.08	-0.00755±0.13	-0.00561±2.80
50	73.34±0.06	-0.00461±0.06	-0.00339±1.69	72.65±0.06	-0.01261±0.22	-0.00947±4.73
60	42.17±0.05	-0.00941±0.12	-0.00702±3.51	42.02±0.05	-0.02167±0.43	-0.01617±8.09
70	22.33±0.04	-0.01991±0.31	-0.01482±7.41	22.13±0.04	-0.04158±1.20	-0.03094±15.49
80	11.25±0.04	-0.04568±0.87	-0.03465±17.34	11.05±0.03	-0.08586±3.72	-0.0639±32.10

TABLE 5: Values of N_{part}, $\nu_{[+-,dyn]}$, and $\nu^{corr}_{[+-,dyn]}$ for $^{208}Pb - ^{208}Pb$ collisions at 2.76 TeV [data from [17]].

cent.%	N_{part}	$\nu_{[+-,dyn]}$	$\nu^{corr}_{[+-,dyn]}$
5	382.80±3.1	-0.00104±0.00001	-0.00093±0.00001
10	329.70±4.6	-0.00126±0.00001	-0.00113±0.00002
20	260.50±4.4	-0.00165±0.00001	-0.00148±0.00001
30	186.40±3.9	-0.00236±0.00001	-0.00211±0.00002
40	128.90±3.3	-0.00348±0.00008	-0.00311±0.00008
50	85.00±2.6	-0.00541±0.00004	-0.00483±0.00004
60	52.80±2.0	-0.00903±0.00007	-0.00802±0.00007
70	30.00±2.8	-0.01675±0.00017	-0.01482±0.00017
80	15.80±3.8	-0.03547±0.00041	-0.03144±0.00041

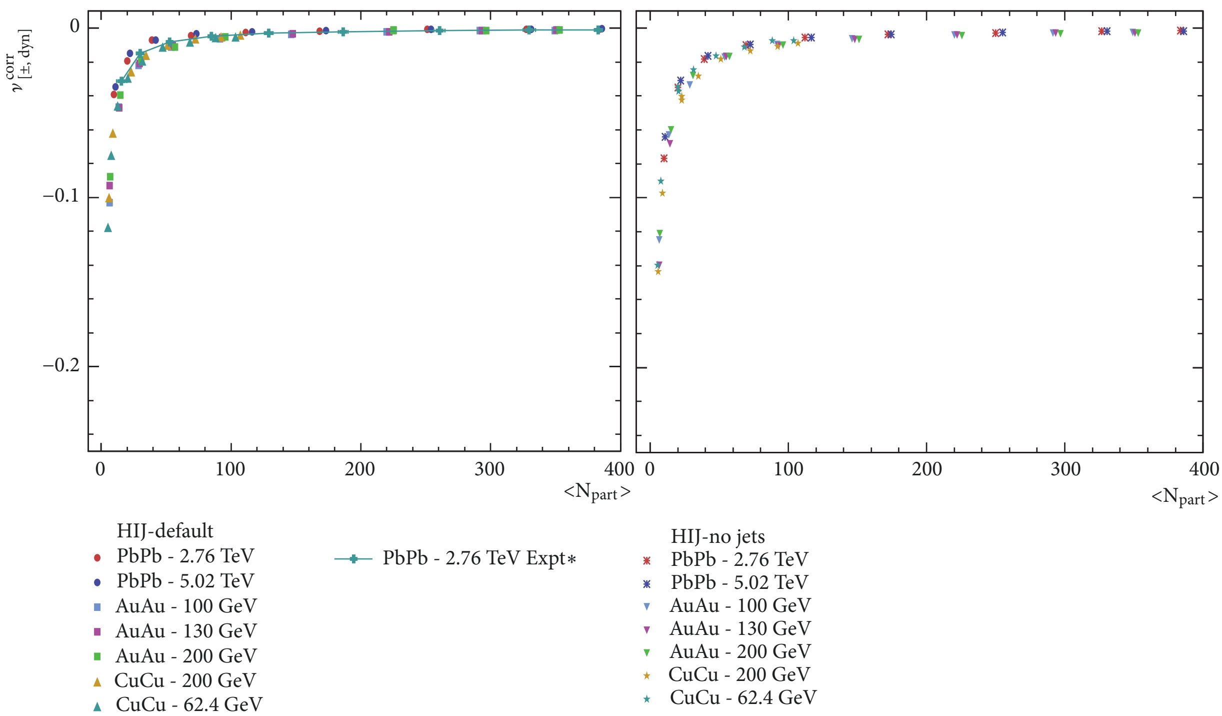

FIGURE 2: The same plot as Figure 1 but for corrected versions of net charge fluctuations.

cause the reduction in the strengths of correlations and fluctuations [37].

The parameter D and $\nu_{[+-,dyn]}$ are related to each other as per the relation

$$\langle N_{ch} \rangle \, \nu_{[+-,dyn]} = D - 4 \qquad (8)$$

The magnitude of net charge fluctuations is limited by the global charge conservation of the produced particles [29]. Considering the effect of global charge conservation, the dynamical fluctuations need to be corrected by a factor of $-4/\langle N_{total} \rangle$, where N_{total} denotes the total charged particle multiplicity of an event in full phase space. Taking into account the global charge conservation and finite acceptance, the corrected value of $\nu_{[+-,dyn]}$ is given by

$$\nu^{corr}_{[+-,dyn]} = \nu_{[+-,dyn]} + \frac{4}{\langle N_{total} \rangle} \qquad (9)$$

Values of $\nu^{corr}_{[+-,dyn]}$ for various data sets are presented in the last column of Tables 2–4, whereas variations of $\nu^{corr}_{[+-,dyn]}$ with N_{part} for these data sets are displayed in Figure 2. Although the trends of variations of $\nu_{[+-,dyn]}$ and $\nu^{corr}_{[+-,dyn]}$ with N_{part} for both types of HIJING events are similar, it might be noticed that the data points corresponding to various energies lie rather close to each other in the semicentral and peripheral collision regions. This weakening of energy dependence is observed for both types of HIJING samples considered.

The observed dependence of $\nu_{[+-,dyn]}$ or its corrected form $\nu^{corr}_{[+-,dyn]}$ on N_{part} or collision centrality indicates the weakening of correlations among the produced hadrons, as one moves from central to peripheral collisions, and nearly matches with the experimental results. These findings, thus, tend to suggest that $\nu_{[+-,dyn]}$ should be proportional to the centrality of collisions or charged particle multiplicity, if AA

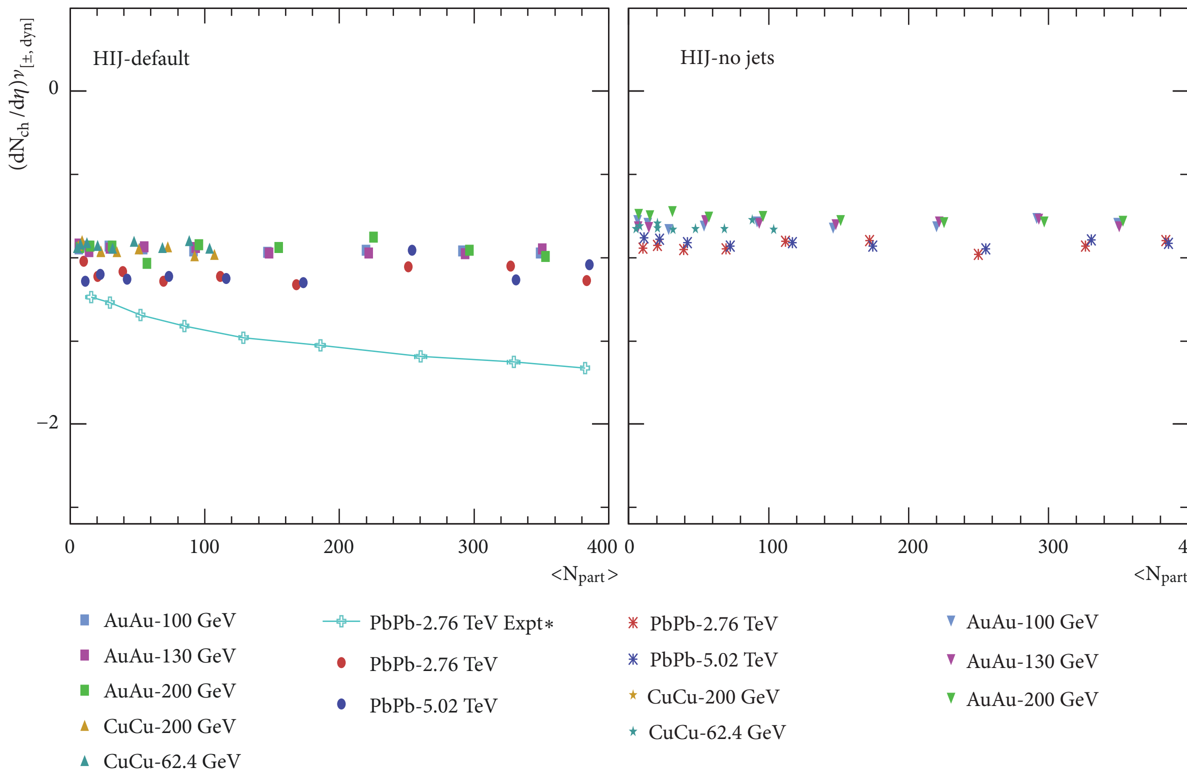

FIGURE 3: $(dN_{ch}/d\eta)\nu_{[+-,dyn]}$ plotted against N_{part} for HIJING default with jet production on (left panel) and jet production off (right panel). The line represents the Pb-Pb data from [17].

collisions are taken as the superpositions of independent nucleon-nucleon (nn) collisions with negligible rescattering effects (which is the basic property of HIJING model). This may be tested by scaling $\nu_{[+-,dyn]}$ by charged particle density $dN_{ch}/d\eta$ and plotting against N_{part}. These plots are displayed in Figures 3 and 4. It may be observed from these figures that the data at different energies show the same qualitative behavior. The values of product $(dN_{ch}/d\eta)\nu_{[+-,dyn]}$ are noticed to be minimum for peripheral collisions and gradually increase to their maximum for the most central collisions; the rise from minimum to maximum is about ~35 - 40 % for various data sets. An increase of 50% has been observed [36] in STAR Au-Au collisions. Such an increase in $(dN_{ch}/d\eta)\nu_{[+-,dyn]}$ values with N_{part} may be accounted to the increase in the particle multiplicity per participant. Data from UA1 and PHOBOS show that, for pp and Au-Au collisions at 200 GeV, $dN_{ch}/d\eta$ increases from 2.4 to 3.9 for most central collisions, thus giving an increase of about 60% [38]

The scaling of $\nu_{[+-,dyn]}$ with N_{part} has also been checked and the plots are shown in Figure 5, whereas after applying the corrections to $\nu_{[+-,dyn]}$ the values of the products are plotted against N_{part} in Figure 6. It is observed from these figures that, with increasing N_{part}, $N_{part}\nu_{[+-,dyn]}$ values gradually decrease for all the data sets. Moreover, for a given N_{part}, the values of product $N_{part}\nu_{[+-,dyn]}$ decrease with the beam energy. It is interesting to note that the difference in the values observed at RHIC and LHC energies, after applying the corrections to $\nu_{[+-,dyn]}$ values, almost vanishes. It is also interesting to note that the HIJING simulated data points lie closer to the corresponding ones reported earlier using the ALICE data [17]. The decreasing trends of $N_{part}\nu_{[+-,dyn]}$ (or $N_{part}\nu^{corr}_{[+-,dyn]}$) from peripheral to most central collisions observed in STAR are in contrast to what is observed in the present study using the HIJING data at RHIC and higher energies. Furthermore, the lower values of product $(dN_{ch}/d\eta)\nu_{[+-,dyn]}$ or $N_{part}\nu_{[+-,dyn]}$, as shown in Figures 4 and 6 predicted by the HIJING with no jets in comparison to those predicted by HIJING-default, indicate the reduction in magnitude of $\nu_{[+-,dyn]}$ due to the productions of jets and minijets.

The variations of $\nu_{[+-,dyn]}$ and $\nu^{corr}_{[+-,dyn]}$ with charged particle density $dN_{ch}/d\eta$ for the two sets of HIJING events are shown in Figure 7. Results based on Pb-Pb 2.76 TeV experimental data [17] for the same η and p_T cuts are also presented in the same figure. It is worthwhile to note in these figures that HIJING-default predicted values for 2.76 TeV data are quite close to the corresponding experimental values. Although the magnitude of $\nu_{[+-,dyn]}$ or $\nu^{corr}_{[+-,dyn]}$ exhibits an energy dependence, which becomes more pronounced as the $dN_{ch}/d\eta$ values decrease, that is, from semicentral to peripheral collisions, the data points for various event samples tend to fall on a single curve. Data for the events with no jets exhibit almost similar behavior except for Pb-Pb data at 2.76 and 5.02 TeV without jet production. This may lead to the conclusion that as one moves from RHIC

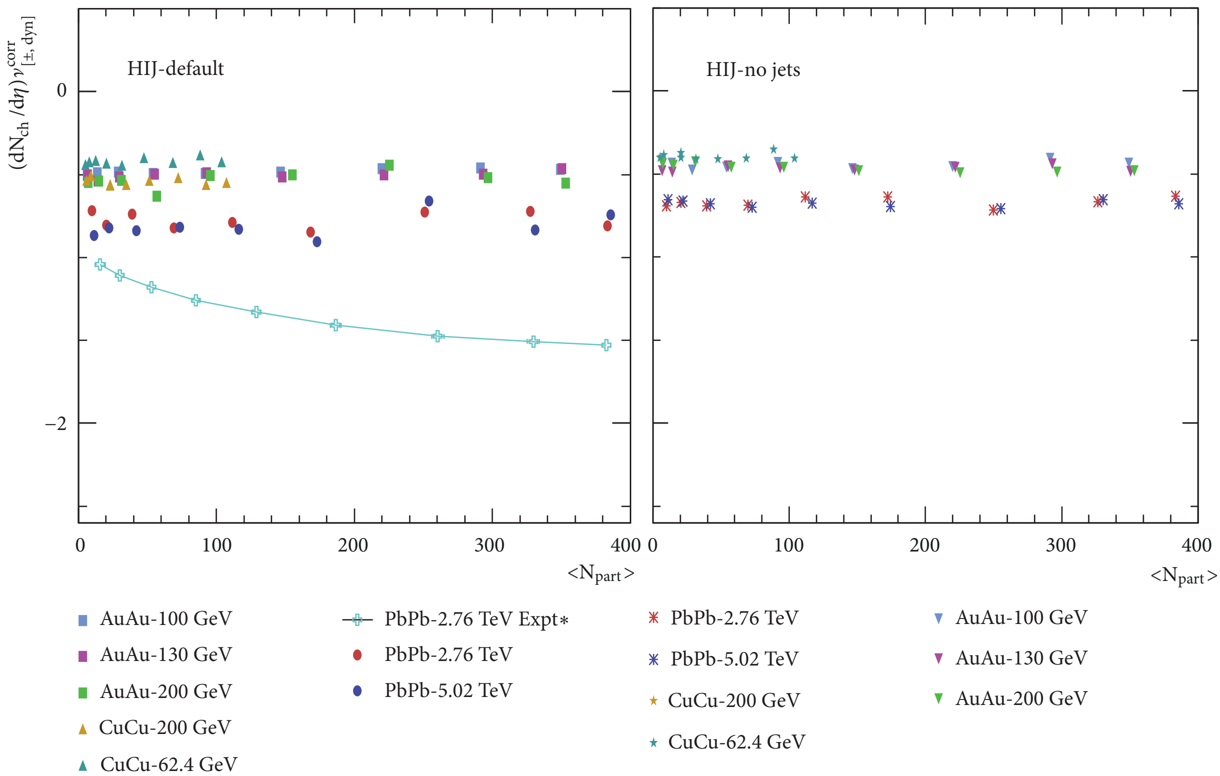

FIGURE 4: The same plot as Figure 3 but for corrected net charge fluctuations, $\nu^{corr}_{[+-,dyn]}$.

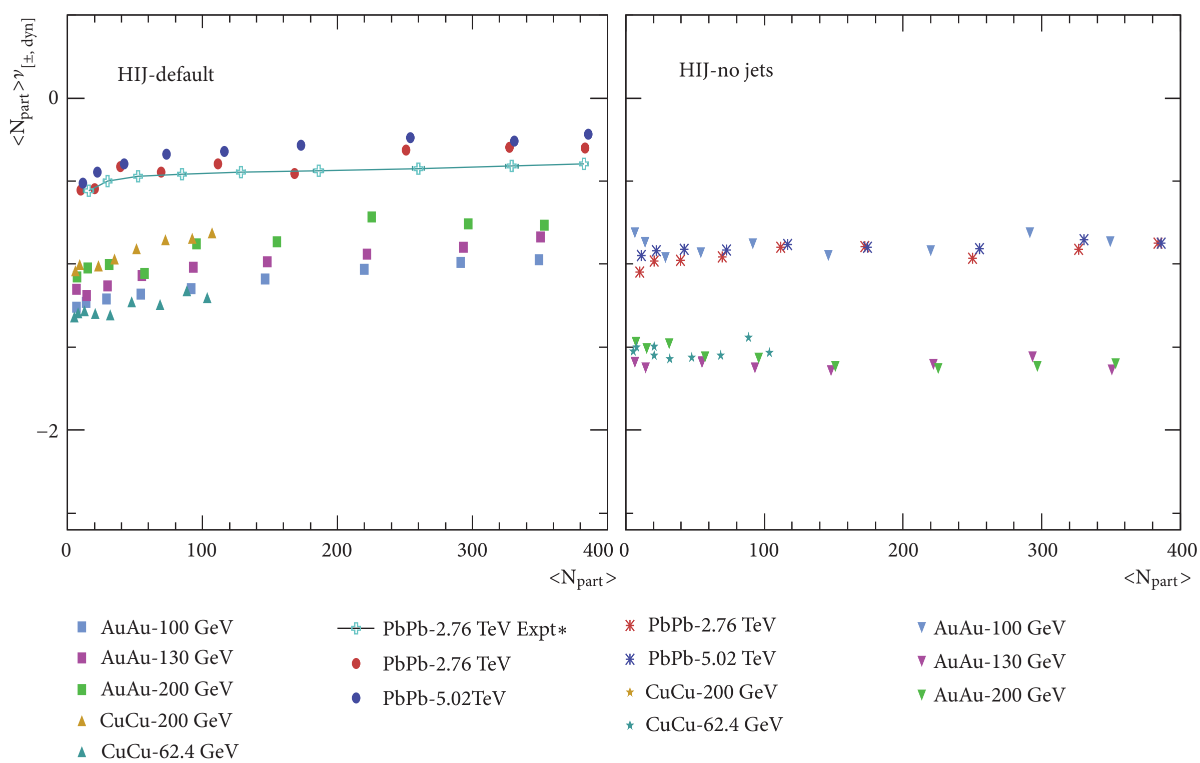

FIGURE 5: Dependence of product of N_{part} and $\nu_{[+-,dyn]}$ on centrality for the two sets of HIJING events at different energies. The line represents the experimental result reported in [17] for $\sqrt{s_{NN}} = 2.76$ TeV Pb-Pb collisions.

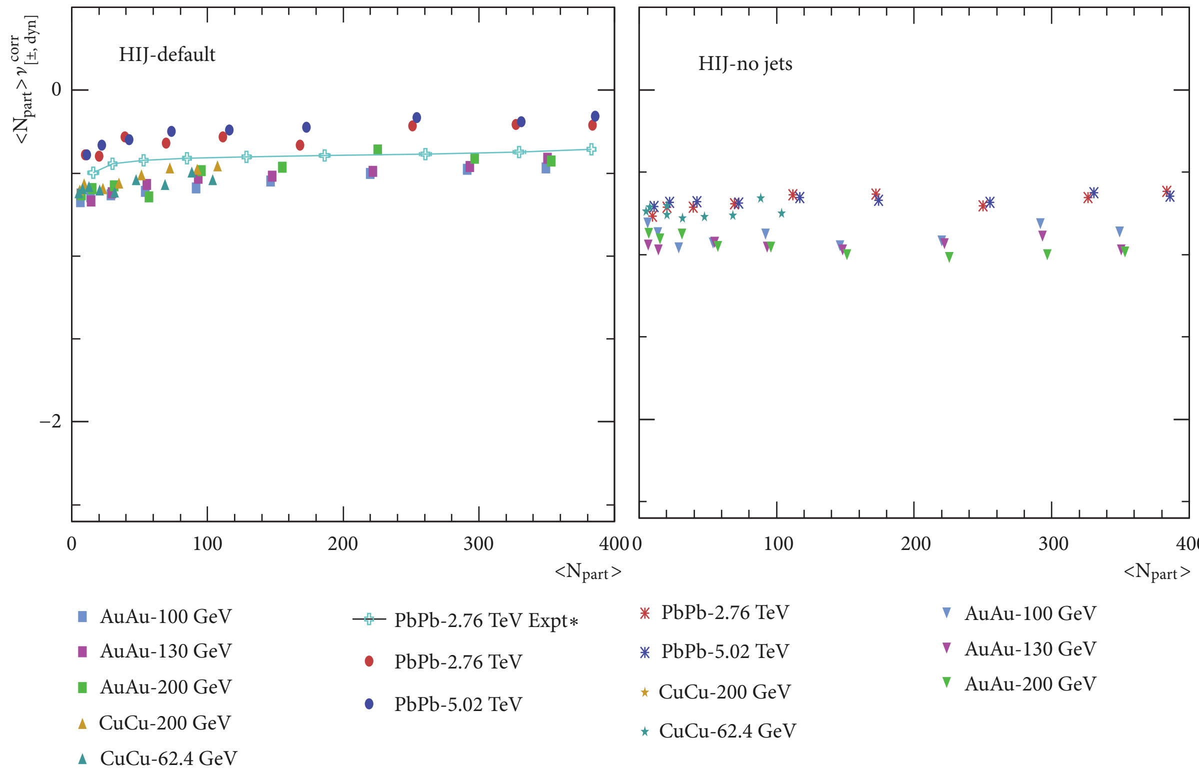

FIGURE 6: Variations of $(N_{part})\nu^{corr}_{[+-,dyn]}$ with N_{part} for the two sets of HIJING events.

to LHC energies, contributions to the particle multiplicity coming from the jet/minijet production cause the reduction in the magnitude of charge fluctuations.

As mentioned earlier, if AA collisions are the superpositions of m number of nn collisions the single particle density for nn and AA collisions would be written as $\rho_1^n n(\eta) = dN_{ch}/d\eta$ and $\rho_1^A A(\eta) = m\rho_1^{nn}\eta$. In such a scenario, the invariant cross section is proportional to the number of nn collisions, m, and the quantity $(dN_{ch}/d\eta)\nu_{[+-,dyn]}$ is independent of centrality of collision and the system size [12]. STAR results, however, give ∼40% increase in $(dN_{ch}/d\eta)\nu_{[+-,dyn]}$ values for Au-Au and Cu-Cu collisions. The product $(dN_{ch}/d\eta)\nu_{[+-,dyn]}$ is plotted against $dN_{ch}/d\eta$ for the two types of event sample in Figure 8. Similar plots for $\nu^{corr}_{[+-,dyn]}$ are also shown in Figure 9. The scaled values of $\nu_{[+-,dyn]}$ and $\nu^{corr}_{[+-,dyn]}$ are observed to increase with increasing $dN_{ch}/d\eta$ values in almost similar fashion. Furthermore, for a given $dN_{ch}/d\eta$ the scaled values of $\nu_{[+-,dyn]}$ or its corrected version are noticed to increase with increasing energy. It is also observed that for a particular set of events (HIJING-default and jets off) the values of $\nu_{[+-,dyn]}$ and $\nu^{corr}_{[+-,dyn]}$ are somewhat larger when jet/minijet production is switched off.

It has been suggested [39] that any multiplicity scaling should be based on the mean multiplicities of charged particles. In the model-independent sources [40], mean particle multiplicity is taken to be proportional to the number of sources, $\langle N_s\rangle$, which changes from event to event. The multiplicity of positively and negatively charged particles may be expressed as

$$\langle N_+\rangle = \alpha_1 + \alpha_2 + \cdots + \alpha_{N_s} \tag{10}$$

$$\langle N_-\rangle = \beta_1 + \beta_2 + \cdots + \beta_{N_s} \tag{11}$$

where α_i and β_i represent the contributions from i^{th} source. The first and second moments of multiplicity distributions are written as

$$\langle N_a\rangle = \langle\alpha\rangle\langle N_s\rangle \tag{12}$$

$$\langle N_b\rangle = \langle\beta\rangle\langle N_s\rangle \tag{13}$$

$$\langle N_a^2\rangle = \langle\alpha^2\rangle\langle N_s\rangle + \langle\alpha\rangle^2\left[\langle N_s^2\rangle - \langle N_s\rangle\right] \tag{14}$$

$$\langle N_b^2\rangle = \langle\beta^2\rangle\langle N_s\rangle + \langle\beta\rangle^2\left[\langle N_s^2\rangle - \langle N_s\rangle\right] \tag{15}$$

$$\langle N_aN_b\rangle = \langle\alpha\beta\rangle\langle N_s\rangle + \langle\alpha\rangle\langle\beta\rangle\langle N_s^2\rangle - \langle N_s\rangle] \tag{16}$$

and here $\langle\alpha\rangle$ and $\langle\beta\rangle$ and $\langle\alpha^1\rangle$, $\langle\beta^1\rangle$, and $\langle\alpha\beta\rangle$ are the first and second moments of the probability distributions $P(\alpha,\beta)$ for a single source.

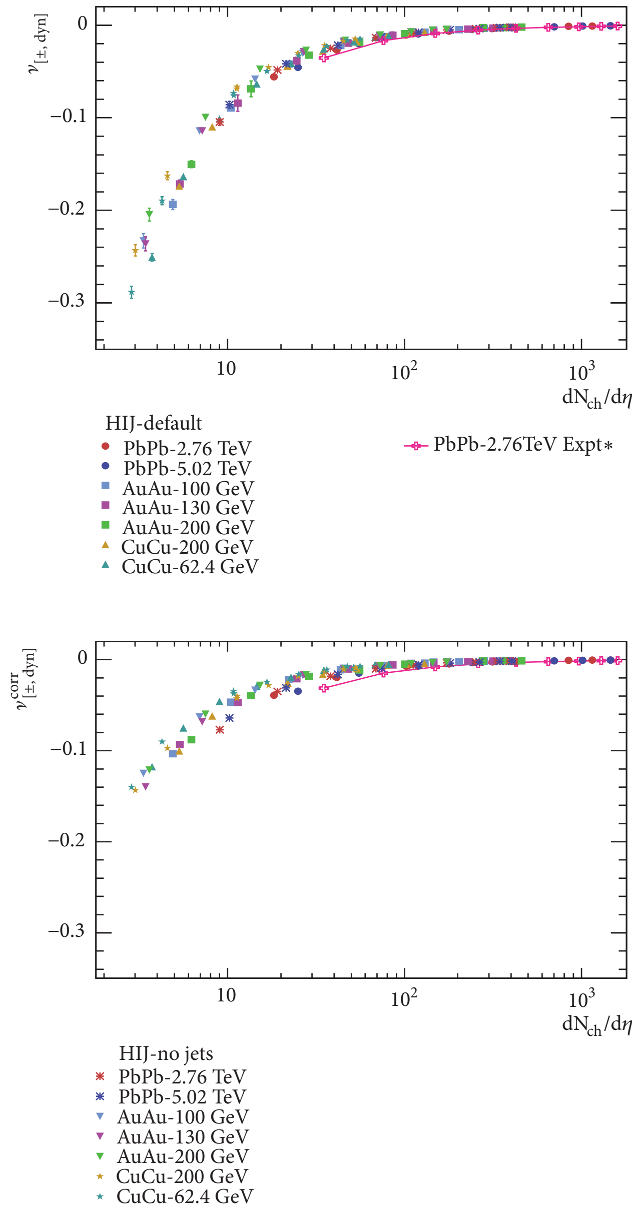

FIGURE 7: Variations of net charge fluctuations $\nu_{[+-,dyn]}$ and their corrected version, $\nu^{corr}_{[+-,dyn]}$, with charged particle density, $dN_{ch}/d\eta$, for the two sets of HIJING events. The lines are due to the 2.76 TeV Pb-Pb values taken from [17].

Following the details as given in [40] and using the equation

$$\nu_{dyn}[a,b] = \frac{\langle N_a^2\rangle}{\langle N_a\rangle^2} + \frac{\langle N_b^2\rangle}{\langle N_b\rangle^2} - 2\frac{\langle N_a N_b\rangle}{\langle N_a\rangle\langle N_b\rangle} - \left(\frac{1}{\langle N_a\rangle} + \frac{1}{\langle N_b\rangle}\right) \quad (17)$$

the following form of ν_{dyn} may be obtained [41]:

$$\nu_{dyn}[a,b] = \frac{1}{\langle N_s\rangle}\left[\frac{\langle\alpha^2\rangle}{\langle\alpha\rangle^2} + \frac{\langle\beta^2\rangle}{\langle\beta\rangle^2} - 2\frac{\langle\alpha\beta\rangle}{\langle\alpha\rangle\langle\beta\rangle} - \left(\frac{1}{\langle\alpha\rangle} + \frac{1}{\langle\beta\rangle}\right)\right] \simeq \frac{1}{\langle N_s\rangle}\nu^*[\alpha,\beta] \quad (18)$$

where $\nu^*[\alpha,\beta]$ is the quantity of the multiplicities of types a and b for each source. This gives $\nu_{a,b}$ to be inversely proportional to the size of the colliding nuclei. On the other hand, as the term $\langle N_s^2\rangle - \langle N_s\rangle$ is canceled out by construction, ν_{dyn} is independent of the system size but requires an additional scaling due to the remaining term, $1/\langle N_s\rangle$. If $1/(1/\langle N_a\rangle + 1/\langle N_b\rangle)$ type of scaling is used, then, substituting (12) and (13) in (17), the term $1/\langle N_s\rangle$ vanishes and the following form of the scaling is obtained:

$$\frac{\nu_{dyn}[a,b]}{1/\langle N_a\rangle + 1/\langle N_b\rangle} = \frac{\nu_{dyn}[\alpha,\beta]}{1/\langle\alpha\rangle + 1/\langle\beta\rangle} \quad (19)$$

The scaling of this type has been tested and the results for the various data sets are shown in Figures 10 and 11. It may be seen in these figures that the scaled $\nu_{[+-,dyn]}$ values for a given energy are nearly independent of charged particle density. It is further observed that the magnitude of scaled $\nu_{[+-,dyn]}$ values increases as one moves from RHIC to LHC energies. The magnitude of $\nu_{[+-,dyn]}$ is observed to be inversely proportional to the number of subcollisions leading to the particle production. If number of particles produced in each subcollision is independent of collision centrality, $\nu_{[+-,dyn]}$ would exhibit $1/N$ scaling [42]. It has been reported [42] that in Au-Au collisions at 130 GeV $1/N$ scaling is clearly noted by the data. HIJING simulated data, however, supports such scaling. In contrast to this, findings from URQMD simulations do not support $1/N$ scaling, which maybe because in URQMD rescattering effects are included which would reduce the magnitude of $N\nu_{[+-,dyn]}$ for central collisions [42]. On the basis of various types of scaling of $\nu_{[+-,dyn]}$ tested in the present study and also the ones by other workers, it may be concluded here that $1/(1/\langle N_a\rangle + 1/\langle N_b\rangle)$ scaling of $\nu_{[+-,dyn]}$ is relatively a better scaling as compared to other scalings.

4. Conclusions

A systematic study of various aspects of net charge fluctuations has been looked into by simulating the Monte Carlo events using the HIJING generator in two different modes, (i) HIJING-default with jet-quenching turned off and (ii) production of jets and minijets turned off. Although both types of events exhibit almost similar dependence of $\nu_{[+-,dyn]}$ on collision centrality and charged particle density, the observed difference in the magnitude of fluctuations clearly reflects the role of jets and minijets in reduction of net charge fluctuations. The trend of energy dependence of ν_{dyn}, for various centrality bins, exhibited by the MC data used in the present study, matches with STAR and ALICE results. N_{part} and $dN_{ch}/d\eta$ scalings of $\nu_{[+-,dyn]}$ after applying the correction for global charge conservation are approximately exhibited by both types of event samples used. This is expected as, in HIJING case, AA collisions are treated as the superpositions

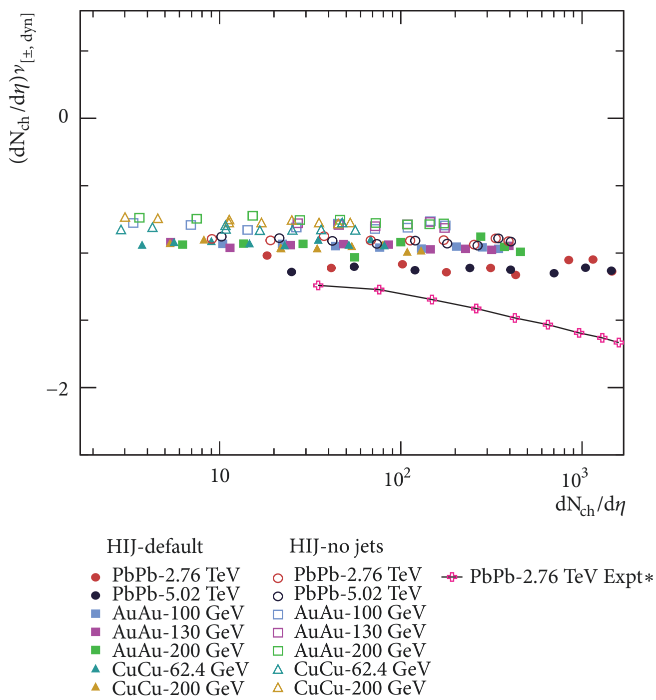

FIGURE 8: Scaling of $\nu_{[+-,dyn]}$ with $dN_{ch}/d\eta$ for various MC data samples at different energies.

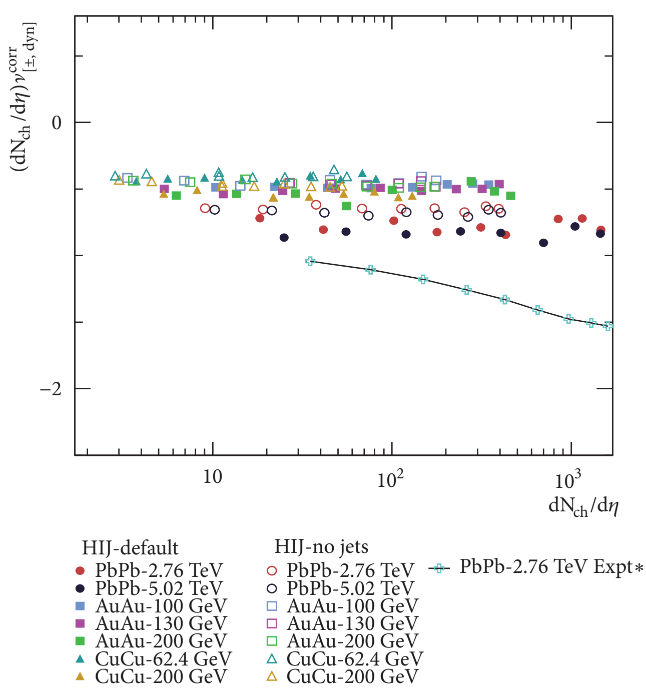

FIGURE 9: The same plot as in Figure 8 but after applying corrections to $\nu_{[+-,dyn]}$ values.

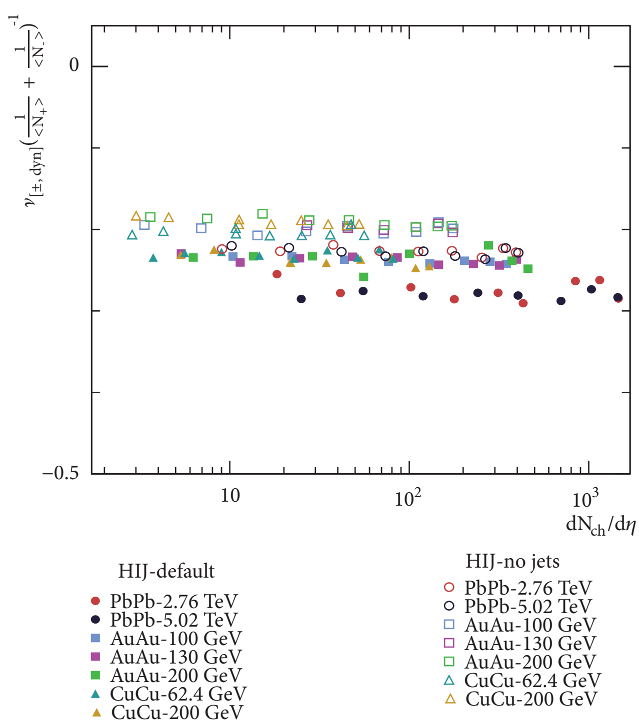

FIGURE 10: $1/(1/\langle N_+\rangle + 1/\langle N_-\rangle)$ scaling of net charge fluctuations at different energies for the two sets of HIJING events.

of multiple nucleon-nucleon collisions. The findings also reveal that the production of jets and minijets plays dominant role in reducing the strength of particle correlations and fluctuations.

Data Availability

The data used to support the findings of this study are available from the corresponding author upon request.

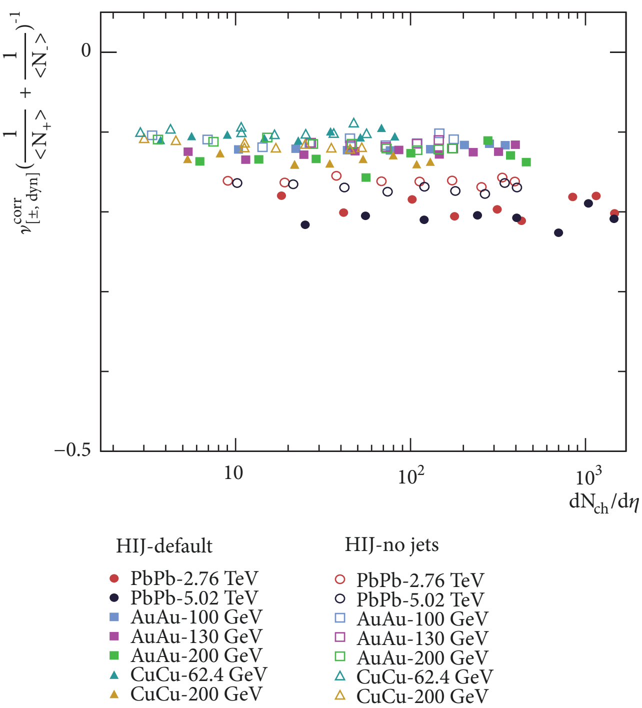

FIGURE 11: $1/(1/\langle N_+\rangle + 1/\langle N_-\rangle)$ scaling of corrected net charge fluctuations for two types of HIJING events at different energies.

Conflicts of Interest

The authors declare that there are no conflicts of interest.

References

[1] E. A. De Wolf, I. M. Dremin, and W. Kittel, "Scaling laws for density correlations and fluctuations in multiparticle dynamics," *Physics Reports*, vol. 270, pp. 1–141, 1996.

[2] S. Ahmad, S. Khan, A. Kumar, A. Singh, A. Ahmad, and B. K. Singh, "Correlations and event-by-event fluctuations in high multiplicity events produced in ^{208}Pb-^{208}Pb collisions," *Advances in High Energy Physics*, vol. 2018, Article ID 6914627, 11 pages, 2018.

[3] R. C. Hwa, "Fractal measures in multiparticle production," *Physical Review D*, vol. 41, no. 5, p. 1456, 1990.

[4] S. Ahmad, A. R. Khan, M. Zafar, and M. Irfan, "On multifractality and multifractal specific heat in ion-ion collisions," *Chaos, Solitons & Fractals*, vol. 42, no. 1, pp. 538–547, 2009.

[5] S. Khan and S. Ahmad, "Multifractal characteristics of multiparticle production in heavy-ion collisions at SPS energies," *International Journal of Modern Physics E*, vol. 27, no. 1, Article ID 1850004, 2018.

[6] A. Bialas and R. Peschanski, "Moments of rapidity distributions as a measure of short-range fluctuations in high-energy collisions," *Nuclear Physics B*, vol. 273, no. 3-4, pp. 703–718, 1986.

[7] R. C. Hwa, "Beyond intermittency: erraticity," *Acta Physica Polonica B*, vol. 27, pp. 1789–1800, 1996.

[8] M. L. Cherry and KLM Collaboration, "Event-by-event analysis of high multiplicity Pb (158-GeV/nucleon) Ag/Br collisions," *Acta Physica Polonica B*, vol. 29, pp. 2129–2146, 1998.

[9] K. Fialkowski and R. Wit, "Event-by-event cluster analysis of final states from heavy ion collisions," *Acta Physica Polonica B*, vol. 30, pp. 2759–2765, 1999.

[10] B. Sharma, M. M. Aggarwal, N. R. Sahoo, and T. K. Nayak, "Dynamical charge fluctuations in the hadronic medium," *Physical Review C*, vol. 91, no. 2, Article ID 024909, 2015.

[11] M. Mukherjee, S. Basu, S. Choudhury, and T. K. Nayak, "Fluctuations in charged particle multiplicities in relativistic heavy-ion collisions," *Journal of Physics G: Nuclear and Particle Physics*, vol. 43, no. 8, Article ID 085102, 2016.

[12] S. Gosh, P. Mali, and A. Mukhopadhyay, "Net-charge fluctuation in Au+Au collisions at energies available at the facility for antiproton and Ion Research using the UrQMD model," *Physical Review C*, vol. 96, no. 2, Article ID 024912, 2017.

[13] S. Jeon and V. Koch, "Fluctuations of particle ratios and the abundance of hadronic resonances," *Physical Review Letters*, vol. 83, no. 26, p. 5435, 1999.

[14] H. Heiselberg and A. D. Jackson, "Anomalous multiplicity fluctuations from phase transitions in heavy ion collisions," *Physical Review C: Nuclear Physics*, vol. 63, Article ID 064904, 2001.

[15] S. Jeon and V. Koch, "Charged particle ratio fluctuation as a signal for quark-gluon plasma," *Physical Review Letters*, vol. 85, no. 10, p. 2076, 2000.

[16] M. Bleicher, S. Jeon, and V. Koch, "Event-by-event fluctuations of the charged particle ratio from nonequilibrium transport theory," *Physical Review C*, vol. 62, no. 6, Article ID 061902, 2000.

[17] B. Abelev and ALICE Collaboration, "Net-charge fluctuations in Pb-Pb collisions at $\sqrt{s_{NN}} = 2.76$ TeV," *Physical Review Letters*, vol. 110, no. 15, Article ID 1523201, 2013.

[18] B. Mohanty, J. Alam, and T. K. Nayak, "Evolution of fluctuation in relativistic heavy-ion collisions," *Physical Review C: Nuclear Physics*, vol. 67, no. 2, Article ID 024904, 2003.

[19] E. V. Shuryak and M. A. stephanov, "Long-range charge fluctuations and search for a quark-gluon plasma signal," *Physical Review C*, vol. 63, no. 6, Article ID 064903, 2001.

[20] M. A. Aziz and S. Gavin, "Causal diffusion and the survival of charge fluctuations in nuclear collisions," *Physical Review C: Nuclear Physics*, vol. 70, Article ID 034905, 2004.

[21] M. Sakaida, M. Asakawa, and M. Kitazawa, "Effects of global charge conservation on time evolution of cumulants of conserved charges in relativistic heavy ion collisions," *Physical Review C*, vol. 90, no. 6, Article ID 064911, 2014.

[22] M. Prakash, R. Rapp, J. Wambach, and I. Zahed, "Isospin fluctuations in QCD and relativistic heavy-ion collisions," *Physical Review C*, vol. 65, no. 3, Article ID 034906, 2002.

[23] M. R. Atayan, B. Yuting, E. A. De Wolf et al. et al., "Charge fluctuations in π^+p and K$^+$p collisions at 250 GeV/c," *Physical Review D: Particles, Fields, Gravitation and Cosmology*, vol. 71, no. 1, Article ID 012002, 2005.

[24] S. Jeon and V. Koch, "Event-by-event fluctuations," in *Koch in Quark-Gluon Plasma3*, R. C. Hwa and X. N. Wang, Eds., p. 430, World Scientific, Singapore, 2004, https://arxiv.org/abs/hep-ph/0304012.

[25] S. A. Voloshin, "Transverse radial expansion in nuclear collisions and two particle correlations," *Physics Letters B*, vol. 632, no. 4, pp. 490–494, 2006.

[26] J. Zarnek, "Measures of charge fluctuations in nuclear collisions," *Physical Review C*, vol. 66, no. 2, Article ID 024905, 2002.

[27] B. J. Abelev and STAR Collaboration, "Beam-energy and system-size dependence of dynamical net charge fluctuations," *Physical Review C*, vol. 79, no. 2, Article ID 024906, 2009.

[28] K. Adox and PHENIX Collaboration, "Net charge fluctuations in Au + Au interactions at $\sqrt{sNN} = 130$ GeV," *Physical Review Letters*, vol. 89, no. 8, Article ID 082301, 2002.

[29] C. A. Pruneau, S. Gavin, and S. Voloshin, "Methods for the study of particle production fluctuations," *Physical Review C*, vol. 66, no. 4, Article ID 0444904, 2002.

[30] L. Foà, "Inclusive study of high-energy multiparticle production and two-body correlations," *Physics Reports*, vol. 22, no. 1, pp. 1–56, 1975.

[31] J. Adamus and STAR Collaboration, "Net charge fluctuations in Au + Au collisions at $\sqrt{sNN} = 130$ GeV," *Physical Review C*, vol. 68, no. 4, Article ID 044905, 2003.

[32] Z. You, W. Ke-Jun, and L. Feng, "Charged particle fluctuation in Au+Au collision," *Chinese Physics C*, vol. 34, no. 9, pp. 1436–1439, 2018.

[33] M. Gyulassy and X. N. Wang, "HIJING 1.0: a Monte Carlo program for parton and particle production in high energy hadronic and nuclear collisions," *Computer Physics Communications*, vol. 83, no. 2-3, pp. 307–331, 1994.

[34] Q. Liu and T. A. Trainor, "Jet quenching and event-wise mean-p_t fluctuations in Au-Au collisions at $\sqrt{sNN} = 200$ GeV in Hijing-1.37," *Physics Letters B*, vol. 567, no. 3-4, pp. 184–188, 2003.

[35] K. Kajantie, P. V. Landshoff, and J. Lindfors, "Minijet production in high-energy nucleus-nucleus collisions," *Physical Review Letters*, vol. 59, no. 22, p. 2527, 1987.

[36] M. Gyulassy and M. Plumer, "Jet quenching in dense matter," *Physics Letters B*, vol. 243, no. 4, pp. 432–438, 1990.

[37] X. N. Wang, "Mini-jets and multiplicity fluctuation in small rapidity intervals," *Physics Letters B*, vol. 248, no. 3-4, pp. 447–452, 1990.

[38] C. A. Pruneau and STAR Collaboration, "Net charge fluctuations at RHIC," *Acta Physica Hungarica A*, vol. 25, no. 2-4, pp. 401–408, 2006.

[39] V. Koch and T. Schuster, "Energy dependence of K/π fluctuations in relativistic heavy-ion collisions," *Physical Review C: Nuclear Physics*, vol. 81, Article ID 034910, 2010.

[40] A. Biallas, M. Bleszynski, and W. Czyz, "Multiplicity distributions in nucleus-nucleus collisions at high energies," *Nuclear Physics B*, vol. 111, pp. 461–476, 1976.

[41] M. Arslandok and ALICE Collaboration, "Event-by-event identified particle ratio fluctuations in Pb–Pb collisions with alice using the identity method," *Nuclear Physics A*, vol. 956, pp. 870–873, 2016.

[42] C. A. Pruneau and STAR Collaboration, "Event by event net charge fluctuations," *Acta Physica Hungarica A. Heavy Ion Physics*, vol. 21, no. 2–4, pp. 261–266, 2004.